Selected Cysteine Point Mutations Confer Mercurial Sensitivity to the Mercurial-Insensitive Water Channel MIWC/AQP-4[†]

Lan-bo Shi and A. S. Verkman*

Departments of Medicine and Physiology, Cardiovascular Research Institute, University of California, San Francisco, California 94143-0521

Received August 22, 1995; Revised Manuscript Received November 9, 1995[⊗]

ABSTRACT: The mercurial-insensitive water channel (MIWC or AQP-4) is a 30−32 kDa integral membrane protein expressed widely in fluid-transporting epithelia [Hasegawa et al. (1994) *J. Biol. Chem. 269*, 5497−5500]. To investigate the mercurial insensitivity and key residues involved in MIWC-mediated water transport, amino acids just proximal to the conserved NPA motifs (residues 69−74 and 187−190) were mutated individually to cysteine. Complementary RNAs were expressed in *Xenopus* oocytes for assay of osmotic water permeability (P_f) and $HgCl_2$ inhibition dose-response. Oocytes expressing the cysteine mutants were highly water permeable, with P_f values ($24-33 \times 10^{-3}$ cm/s) not different from that of wild-type (WT) MIWC. P_f was reversibly inhibited by $HgCl_2$ in mutants S70C, G71C, G72C, H73C, and S189C but insensitive to $HgCl_2$ in the other mutants. $K_{1/2}$ values for 50% inhibition of P_f by $HgCl_2$ were as follows (in millimolar): 0.40 (S70C), 0.36 (G71C), 0.14 (G72C), 0.45 (H73C), 0.24 (S189C), and >1 for WT MIWC and the other mutants. To test the hypothesis that these residues are near the MIWC aqueous pore, residues 72 and 188 were mutated individually to the larger amino acid tryptophan. P_f in oocytes expressing mutants G72W or A188W ($1.3-1.4 \times 10^{-3}$ cm/s) was not greater than that in water-injected oocytes even though these proteins were expressed at the oocyte plasma membrane as shown by quantitative immunofluorescence. Coinjection of cRNAs encoding WT MIWC and G72W or A188W indicated a dominant negative effect; P_f ($\times 10^{-3}$ cm/s) was 22 (0.25 ng of WT), 10 (0.25 ng of WT + 0.25 ng of G72W), and 12 (0.25 ng of WT + 0.25 ng of A188W). Taken together, these results suggest the MIWC is mercurial-insensitive because of absence of a cysteine residue near the NPA motifs and that residues 70−73 and 189 are located at or near the MIWC aqueous pore. In contrast to previous data for the channel-forming integral protein of 28kDa (CHIP28), the finding of a dominant negative phenotype for mutants G72W and A188W indicates that MIWC monomers interact at a functional level.

Several members of a family of water-transporting proteins (aquaporins) have been identified recently [for review, see Agre et al. (1993), Van Os et al. (1994), and Verkman et al. (1996)]. The water channels are small integral membrane proteins which have homology to the major intrinsic protein of lens fiber (MIP; Reizer et al., 1993). Water channels in mammalian tissues include CHIP28[1] (channel-forming integral protein; Preston & Agre, 1991), WCH-CD (water channel-collecting duct or AQP-2; Fushimi et al., 1993), MIWC (mercurial insensitive water channel; Hasegawa et al., 1994), GLIP (glycerol intrinsic protein or AQP-3; Ma et al., 1994; Ishibashi et al., 1994), and AQP5 (Raina et al., 1995). CHIP28, MIWC, GLIP, and AQP5 are expressed widely in plasma membranes of fluid-transporting epithelia and endothelia, whereas WCH-CD is expressed only in principal cells of the kidney collecting duct. With the exception of MIWC, water channel-mediated water permeability is inhibited by mercurial sulfhydryl reagents such as $HgCl_2$. In CHIP28, residue cysteine 189 has been shown to be the site of mercurial binding and water transport inhibition (Preston et al., 1993; Zhang et al., 1993b). Proteins WCH-CD, GLIP, and AQP5 have cysteine residues at identical locations in their amino acid sequences after alignment with CHIP28. Mutations in WCH-CD are associated with hereditary non-X-linked nephrogenic diabetes insipidus (Deen et al., 1994), whereas mutations in CHIP28 do not cause apparent disease (Preston et al., 1994b). The roles of MIWC, GLIP, and AQP5 in normal physiology and clinical disease have not been established. Various other aquaporins have been identified in nonmammals, including a number of important plant water channels (Maurel et al., 1993; Daniels et al., 1994).

MIWC was cloned from a rat lung cDNA library (Hasegawa et al., 1994) and has 41% amino acid identity to CHIP28. MIWC functions as a water-selective channel at the basolateral membrane of epithelial cells in the kidney-collecting duct, the trachea, small airways, gastric parietal cells, and salivary glands, as well as in brain ependymal and astroglial cells, skeletal myocytes, and ciliary body (Frigeri et al., 1995a,b). An isoform of MIWC (named AQP-4) with a different N-terminus was subsequently cloned from a rat brain cDNA library (Jung et al., 1994a). Like other members of the MIP26 family, MIWC contains two tandem sequence repeats and two conserved NPA motifs. Topology analysis

[†] Supported by NIH Grants DK35125, HL42368, and HL51854.

* Address correspondence to Alan S. Verkman, M.D., Ph.D., 1246 Health Sciences East Tower, Cardiovascular Research Institute, University of California, San Francisco, CA 94143-0521. Phone: (415)-476-8530. Fax: (415)-665-3847.

[⊗] Abstract published in *Advance ACS Abstracts,* December 15, 1995.

[1] Abbreviations: AQP, aquaporin; β-ME, β-mercaptoethanol; CHIP28, channel-forming integral protein of 28 kDa; cRNA, complementary RNA; γTIP, γ-tonoplast intrinsic protein; GLIP, glycerol intrinsic protein; HR, hydrophobic region; MIWC, mercurial-insensitive water channel; P_f, osmotic water permeability coefficient; WCH-CD, water channel-collecting duct; WT, wild-type MIWC.

0006-2960/96/0435-538$12.00/0

Table 1: Oligonucleotides for Site-Directed Mutagenesis of MIWC[a]

I69C	5′ ^{222}GAT GTG GCC ACC GCT [GCA] ATG ACC GAA GCA CTG AAC CA^{185} 3′
S70C	5′ ^{225}GTT GAT GTG GCC ACC [GCA] GAT ATG ACC GAA GCA CTG AAC CA^{185} 3′
G71C	5′ ^{220}T GTG GCC [ACA] GCT GAT GT^{203} 3′
G72C	5′ ^{229}C TGG GTT GAT GTG [GCA] TCC GCT GAT GTG GCC^{199} 3′
G72W	5′ ^{231}CGC TGG GTT GAT GTG [CCA] ACC GCT GAT GTG GCC^{199} 3′
H73C	5′ ^{234}CAC CGC TGG GTT GAT [GCA] GCC ACC GCT GAT GTG^{202} 3′
I74C	5′ ^{232}GT CAC CGC TGG GTT [GCA] GTG GCC ACC GCT GAT^{205} 3′
G187C	5′ ^{577}C TGG ATT CAT GCT GGC [ACA] GGT ATA ATT GAT TGC AAA C^{540} 3′
A188C	5′ ^{577}C TGG ATT CAT GCT [GCA] TCC GGT ATA ATT G^{549} 3′
A188W	5′ ^{580}G AGC TGG ATT CAT GCT [CCA] TCC GGT ATA ATT GAT TGC^{544} 3′
S189C	5′ ^{575}GG ATT CAT [GCA] GGC TCC GG^{557} 3′
M190C	5′ ^{587}AA GGA TCG AGC TGG ATT [GCA] GCT GGC TCC GGT ATA A^{552} 3′

[a] The indicated antisense oligonucleotides were used to generate the MIWC mutations. The mismatched bases are underlined, and codons in brackets represent the mutated amino acid residues. In some cases, additional mismatched bases outside of the brackets leading to silent mutations were created to avoid self-complementary annealing between C-G rich regions. Superscripted numbers represent the base pair number of the MIWC cDNA coding sequence.

indicated that MIWC spans the membrane six times with its N- and C- termini in the cytosol (Shi et al., 1995). Interestingly, although MIWC and CHIP28 (Preston et al., 1994a) have similar topologies at the plasma membrane, their early biogenesis mechanisms at the endoplasmic reticulum differed (Skach et al., 1994; Shi et al., 1995); MIWC utilized a conventional mechanism of polytopic membrane protein biogenesis, whereas CHIP28 initially spans the endoplasmic reticulum membrane four times, becomes membrane-integrated after four hydrophobic residues (HRs) (residues 1−107), and requires HRs 2−4 (residues 35−139) to terminate translocation. Recently, a human mercurial-insensitive water channel which was present as a single copy gene at chromosome locus 18q22 was cloned (Yang et al., 1995). Genomic DNA analysis revealed two distinct but overlapping transcriptional units in which proteins of 30 and 32 kDa are encoded by alternatively spliced mRNAs. Another unique feature of MIWC is the expression of spliced nonfunctional transcripts in which distinct exon segments are absent (Hasegawa et al., 1994; Yang et al., 1995).

A first goal of this study was to test the hypothesis that MIWC is mercurial-insensitive because residue 188 (which corresponds to residue cysteine 189 in CHIP28) is alanine, which does not interact with mercurials, rather than cysteine. Unexpectedly, it was found that mutagenesis of MIWC residue 188 to cysteine (A188C) did not make MIWC mercurial-sensitive, whereas point cysteine mutations at several other residues just proximal to the NPA motifs did convert MIWC to a highly mercurial-sensitive water channel. The hypothesis that these residues are located at or near the MIWC aqueous pathway was supported by experiments showing that mutation of these residues individually to the larger amino acid tryptophan blocked water transport through MIWC. In addition, in contrast to previous studies in which individual CHIP28 monomers within tetramers were found to be functionally independent (Zhang et al., 1993b; Preston et al., 1993; Shi et al., 1994), the MIWC tryptophan mutants suppressed the water permeability of wild-type MIWC.

MATERIALS AND METHODS

Site-Directed Mutagenesis. MIWC mutants were constructed with the Altered Sites II *in vitro* Mutagenesis System (Promega) using expression vector pSP64T-MIWC containing the full-length rat MIWC coding sequence as template (Shi et al., 1995). Table 1 lists the oligonucleotides used to construct the MIWC mutants. The mutated cDNAs were subcloned in vector pSP64T (which contains an upstream *Xenopus* α-globin enhancer sequence; Zhang et al., 1993a) at *Hin*dIII and *Eco*RI restriction sites. WT and mutated MIWC cDNAs were confirmed by DNA sequence analysis.

cRNA Transcription. Complementary RNA was transcribed *in vitro* by SP6 RNA polymerase (Boehringer Mannheim) using 4 μg of plasmid DNA in a 100 μL volume at 37 °C for 2 h. Diguanosine triphosphate (0.5 μM) (Pharmacia LKB Biotechnology Inc.) was included in the reaction mixture for capping. At the completion of the reaction, plasmid DNA was digested with RNase-free DNase (Boehringer Mannheim). After phenol−chloroform extraction and precipitation, the cRNA was washed with 70% ethanol and suspended in distilled water for oocyte injection.

Oocyte Injection and Water Transport Assay. Stage V and VI oocytes from *Xenopus laevis* were isolated and defolliculated with collagenase (Type IA, Sigma, 1 mg/mL for 1 h at 20 °C) in Barth's buffer (200 mosM). Oocytes were microinjected with 50 nL samples of cRNA (0−10 ng/μL) and incubated at 18 °C for 24 h. Osmotic water permeability (P_f, in centimeters per second) was measured from the time course of oocyte swelling at 10 °C in response to a 20-fold dilution of the extracellular Barth's buffer with distilled water (Zhang et al., 1990). In some experiments, $HgCl_2$ was added directly to the assay solution (final concentration of 0.075−1 mM) 20 s after buffer dilution. Oocyte P_f was calculated from the initial rate of swelling, $d(V/V_o)/dt$, by the relation $P_f = [d(V/V_o)/dt]/[(S/V_o)V_w(Osm_{out} - Osm_{in})]$, where $S/V_o = 50$ cm^{-1}, $V_w = 18$ cm^3/mol, and $Osm_{out} - Osm_{in} = 190$ mosM.

Immunofluorescence. Polyclonal antibodies against a C-terminus synthetic peptide of rat MIWC (residues 287−301, EKGKDSSGEVLSSV) were raised in rabbits and affinity purified using an iodoacetyl-cross-linked agarose resin conjugated with the synthetic peptide (Frigeri et al., 1995b). Oocytes were fixed in Barth's buffer containing 4% paraformaldehyde for 4 h, cryoprotected overnight in phosphate-buffered saline (PBS) containing 30% sucrose, embedded in OCT compound, and frozen in liquid N_2. Cryostat sections (4−6 μm) were mounted on Superfrost/Plus microscope slides (Fisher). Slides were washed with 0.5% Triton X-100 for 30 min and incubated for 30 min with PBS containing 1% bovine serum albumin (BSA) and then with purified MIWC antibody (0.3−0.5 μg/mL) for 1 h at 23 °C in PBS containing 1% BSA. Slides were rinsed with PBS and then incubated for 30 min with sheep anti-rabbit IgG

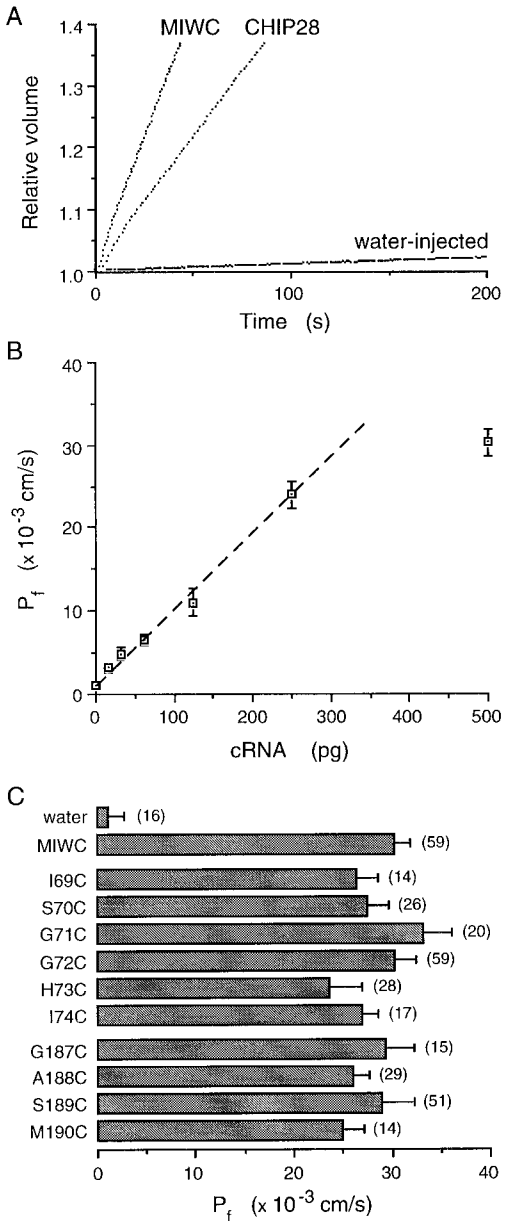

FIGURE 1: Osmotic water permeability in *Xenopus* oocytes expressing wild-type MIWC and cysteine mutants. (A) Time course of oocyte swelling at 10 °C in response to a 20-fold dilution of the extracellular Barth's buffer with distilled water. Oocytes were microinjected with 0.5 ng of cRNA encoding MIWC or CHIP28. (B) Oocyte P_f (SE, 20 oocytes in each group) as a function of the amount of injected cRNA encoding wild-type MIWC. (C) Summary of P_f in oocytes expressing wild-type MIWC and the cysteine mutants. cRNA (0.5 ng) was injected into each oocyte group. Values in parentheses represent the number of oocytes measured in each group.

conjugated with fluorescein (1:50, BRL). Slides were washed three times with PBS and covered with diazabicyclooctane (Dabco) solution to reduce photobleaching and a glass coverslip. Oocytes were imaged with a Leitz epifluorescence microscope equipped with 10× dry objective and a cooled charged coupled device camera (Photometrics) as described previously (Shi et al., 1994; Zen et al., 1992). Background-subtracted fluorescence per unit length of oocyte plasma membrane was quantified in multiple membrane-containing regions of each oocyte. At least 20 oocytes were measured on two to four separate slides for each condition. The slides were processed identically and on the same day for immunostaining and image acquisition studies.

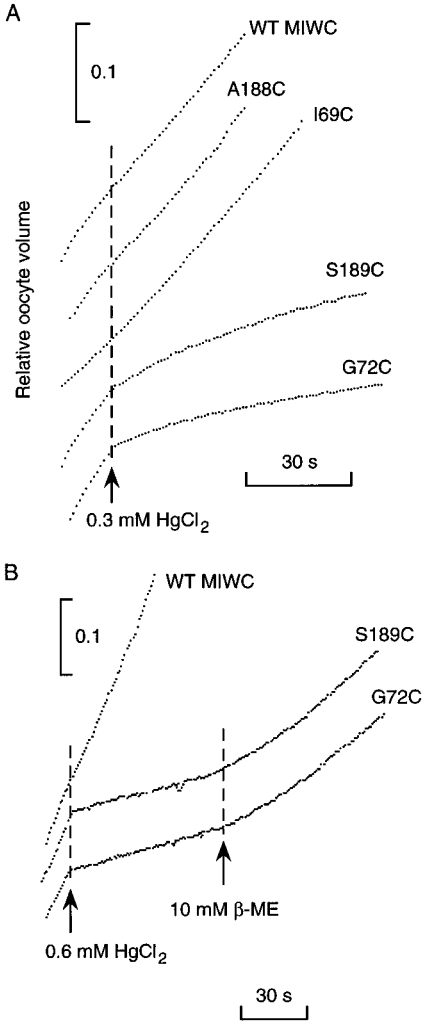

FIGURE 2: Reversible inhibition of MIWC cysteine mutants by $HgCl_2$. (A) Time course of swelling in oocytes injected with 0.5 ng of cRNA encoding wild-type MIWC and indicated cysteine mutants. $HgCl_2$ (final concentration of 0.3 mM) was added at the arrow. (B) Same type of study as in A except for addition of a higher concentration of $HgCl_2$ followed by β-mercaptoethanol.

RESULTS

Figure 1A shows the time course of swelling in *Xenopus* oocytes in response to an osmotic gradient produced by dilution of the extracellular media. Oocytes expressing wild-type MIWC were highly water permeable compared to control (water-injected) oocytes and more water permeable than oocytes injected with an equal quantity of cRNA encoding CHIP28. For very small amounts of injected cRNA, the osmotic water permeability coefficient (P_f) increased linearly with cRNA and reached a maximum value of $(30 \pm 2) \times 10^{-3}$ cm/s with greater than ~300 pg of injected cRNA (Figure 1B). A series of cysteine mutant cDNAs were generated by replacing individual amino acids in MIWC (residues 69−74 and 187−190) with cysteine. Water permeability in oocytes expressing each of the cysteine mutants was high and similar to that of wild-type MIWC (Figure 1C).

The inhibitory effect of $HgCl_2$ on water permeability mediated by wild-type and mutant MIWCs was studied by addition of $HgCl_2$ directly into the assay solution during measurements. Each oocyte thus served as its own control. Water permeability in oocytes expressing S70C, G71C, G72C, H73C, and S189C was remarkably reduced upon

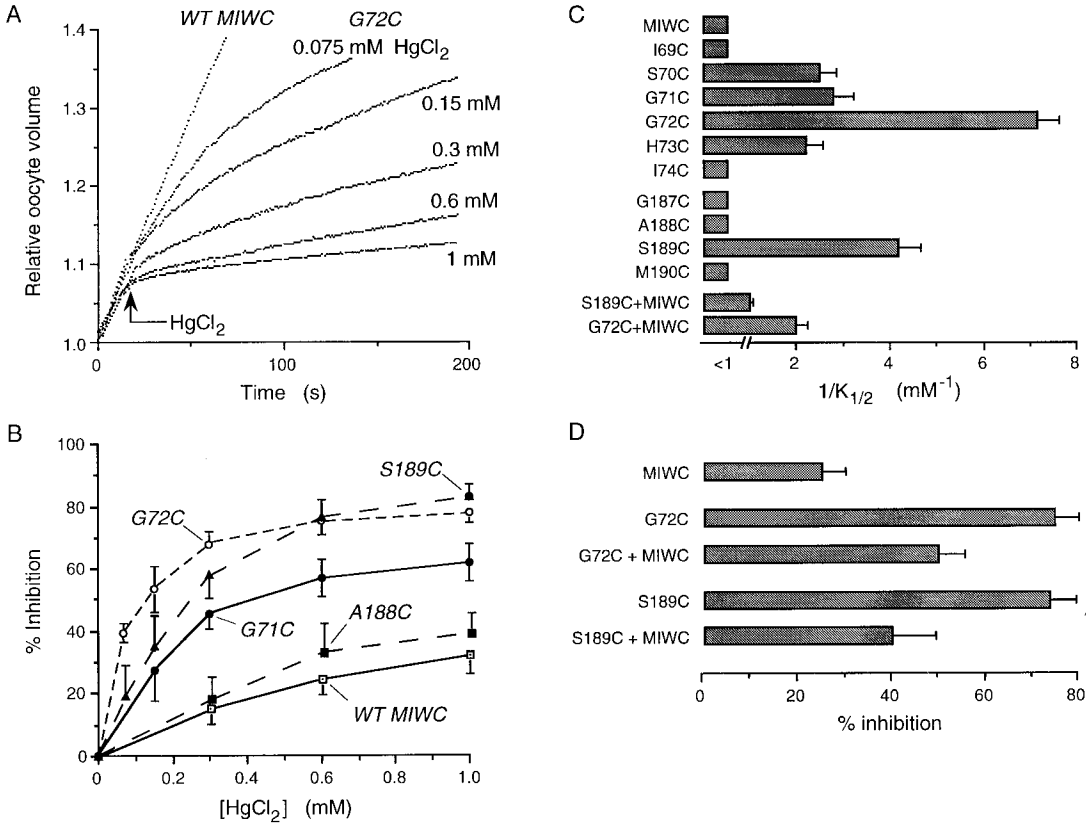

FIGURE 3: Quantitative analysis of $HgCl_2$ inhibition of wild-type MIWC and single-site cysteine mutants. (A) Time course of swelling in oocytes injected with 0.5 ng of cRNA encoding wild-type MIWC and MIWC G72C. $HgCl_2$ (final concentrations indicated) was added at the arrow. (B) Summary of representative dose-response data for $HgCl_2$ inhibition of P_f in oocytes injected with 0.5 ng of indicated cRNAs (SE, 10−20 oocytes for each point). Percentage inhibition was calculated from fitted slopes of oocyte swelling curves before and after $HgCl_2$ addition (Shi et al., 1994). (C) Summary of fitted reciprocal $K_{1/2}$ values from data as in B. (D) $HgCl_2$ sensitivity of oocytes coexpressing wild-type MIWC and mutants G72C or S189C. cRNAs encoding MIWC G72C (0.5 ng), G72C + WT (0.25 + 0.25 ng), S189C (0.5 ng), and S189C + WT (0.25 + 0.25 ng) were expressed in oocytes. P_f inhibition was measured at 0.6 mM $HgCl_2$.

addition of $HgCl_2$. Representative oocyte-swelling data are provided in Figure 2A. There was little effect of $HgCl_2$ in oocytes expressing wild-type MIWC and A188C but prompt inhibition of the swelling rate in oocytes expressing S189C and G72C. Inhibition of water permeability by $HgCl_2$ was reversed significantly by subsequent addition of the reducing agent β-mercaptoethanol as shown by representative swelling curves in Figure 2B.

The mercurial sensitivity for each of the mutant cDNAs was quantified from $HgCl_2$ dose-response studies; oocyte-swelling curves for MIWC G72C are shown in Figure 3A. Dose-response data for wild-type MIWC and several cysteine point mutants are shown in Figure 3B. Figure 3C summarizes results from a full set of dose-response studies. The plotted quantity is $1/K_{1/2}$, which is the reciprocal of the concentration of $HgCl_2$ giving 50% inhibition of P_f. $1/K_{1/2}$ values (in mM^{-1}) are shown because they correlate qualitatively with inhibitory potency. The rank order of $HgCl_2$ sensitivity, from highest to lowest, was G72C > S189C > G71C > S70C > H73C. Interestingly, the mutants G72C and S189C had significantly greater $HgCl_2$ sensitivity than wild-type CHIP28, which when studied in parallel gave a $1/K_{1/2}$ value of ~3 mM^{-1}. The other MIWC mutants were relatively $HgCl_2$-insensitive, with $K_{1/2}$ values exceeding 1 mM, not different from that of wild-type MIWC. $HgCl_2$ concentrations of >1 mM were not used because of toxic effects, as demonstrated by a lack of reversibility by β-mercaptoethanol.

To investigate whether MIWC monomers functioned independently with respect to $HgCl_2$ inhibition, P_f measurements were carried out in oocytes coinjected with equal quantities of cRNAs encoding wild-type and mutant MIWCs. Figure 3C shows that coexpression of wild-type MIWC together with the mutants G72C or S189C caused a decrease in apparent $HgCl_2$ sensitivity. Figure 3D shows the percent inhibition of oocyte P_f at a high concentration of $HgCl_2$ (0.6 mM). The percent inhibition of P_f by $HgCl_2$ for oocytes expressing the two different cRNAs was nearly halfway between those for oocytes expressing wild-type MIWC and the cysteine mutants alone. These results indicate independent functioning of MIWC for $HgCl_2$ inhibition. As reported previously (Hasegawa et al., 1994), it is unclear whether the small percentage of $HgCl_2$ inhibition for wild-type MIWC (30% at 1 mM) (and for several cysteine mutants as shown here) is due to action of $HgCl_2$ at one of the other cysteine residues or to a nonspecific toxic effect of $HgCl_2$; the latter explanation is favored by the incomplete reversal of $HgCl_2$ inhibition at high $HgCl_2$.

The observation that certain residues just proximal to the NPA motifs conferred mercurial sensitivity to MIWC when mutated to cysteine suggested that this region of MIWC may be near the putative aqueous pore. On the basis of previous work in CHIP28 (Zhang et al., 1993b; Preston et al., 1993), it was postulated that mutation of these residues to the larger amino acid tryptophan might produce a water channel with reduced water permeability. The single tryptophan mutants

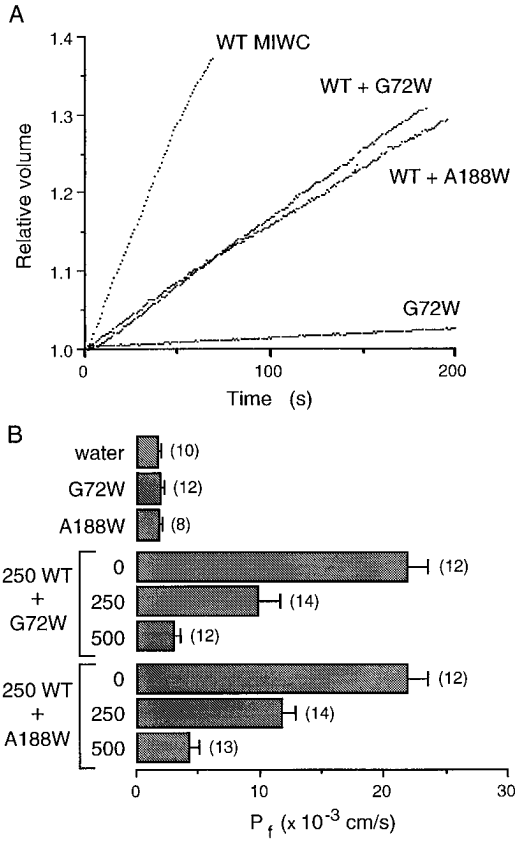

FIGURE 4: Functional analysis of MIWC tryptophan mutations. (A) Time course of swelling in oocytes injected with 0.5 ng of cRNA encoding indicated wild-type MIWC and/or MIWC tryptophan mutants. (B) Summary of P_f values in oocytes injected with cRNAs encoding MIWC G72W or A188C or coinjected with wild-type MIWC (250 pg) and indicated amounts (in picograms) of cRNAs encoding MIWC G72W or A188W.

G72W and A188W were thus generated and studied. Figure 4A,B indicates that water permeability in oocytes expressing these tryptophan mutants was not increased significantly compared to control, indicating either defective protein synthesis (or targeting) and/or reduced intrinsic water permeability of individual MIWC molecules. As quantified in reference to Figure 5 (see below), oocyte immunostaining studies indicated that expression of G72W and A188W is associated with both decreased plasma membrane MIWC protein and decreased intrinsic water permeability compared to oocytes expressing wild-type MIWC. These results support the view that residues just proximal to the NPA motifs in MIWC are important for water channel function.

To determine whether functional and nonfunctional MIWC monomers interact, P_f measurements were carried out in oocytes coinjected with 0.25 ng of cRNA encoding wild-type MIWC and increasing amounts of cRNA encoding the tryptophan mutants G72W or A188W. Figure 4A,B shows that oocyte P_f decreased significantly with increasing amounts of coinjected cRNAs encoding the nonfunctional MIWC tryptophan mutants. The finding of a dominant-negative effect indicates that injection of the mutant cRNAs altered the translation/membrane targeting of wild-type MIWC and/or that wild-type and mutant MIWC monomers interact at the plasma membrane.

Immunofluorescence studies were carried out to evaluate the plasma membrane expression of the various constructs. Figure 5A shows strong immunofluorescence at the plasma membrane of oocytes expressing wild-type MIWC. The signal was weaker with less injected cRNA (Figure 5B) and not above that observed with preadsorbed antibody (not shown) or in water-injected (control) oocytes (Figure 5C). Similar staining was observed for all of the point cysteine mutants (e.g. G72C, Figure 5D), in agreement with the functional data in Figure 1C. Immunostaining of oocytes expressing the tryptophan mutants (e.g. G72W, Figure 5E) was intermediate between those observed for the control (water-injected) oocytes and oocytes expressing wild-type MIWC. By quantitative immunofluorescence, the relative plasma membrane expression (after background subtraction) of various groups of oocytes was 0 (water-injected), 1.0 (0.5 ng of wild-type MIWC), 0.27 ± 0.08 (0.5 ng of G72W), and 0.34 ± 0.1 (0.5 ng of A188W). Similar studies were carried out in oocytes coinjected with cRNA encoding wild-type MIWC and the tryptophan mutants (e.g. G72W + wild-type MIWC, Figure 5F). By quantitative immunofluorescence, relative plasma membrane expression was (in units as above) 0.56 ± 0.07 (0.25 ng of wild-type MIWC + 0.5 ng of A188W) and 0.47 ± 0.09 (0.25 ng of wild-type MIWC + 0.5 ng of G72W). Taken together, these results indicate that the single tryptophan mutants are nonfunctional even though expressed at the oocyte plasma membrane and that expression of a MIWC tryptophan mutant decreases the function of coexpressed wild-type MIWC.

DISCUSSION

Figure 6 shows putative locations of the six cysteine residues in MIWC (residues 54, 65, 84, 101, 156, and 231) along with the conserved NPA motifs and sites at which point cysteine mutations conferred mercurial sensitivity. The assignment of membrane-spanning helical domains is based on hydropathy analysis, sequence alignment, and experimental measurements (Verkman et al., 1996); possible regions of β-structure are not indicated because of insufficient data. The locations of cysteine residues in CHIP28 (residues 87, 102, 152, and 189) and several homologous water-transporting proteins are also indicated. In rat CHIP28, mutation of cysteines 87, 102, and 152, individually or in combinations, did not affect water permeability or inhibition by mercurials, whereas mutation of residue C189 resulted in the loss of mercurial inhibition (Zhang et al., 1993b). Similar results were reported for human CHIP28, which contains cysteine residues at identical positions in its coding sequence (Preston et al., 1993). Figure 6 shows that the various mercurial-sensitive water channels each contain a cysteine residue just proximal to the second NPA sequence, whereas MIWC, and a recently described mercurial-insensitive plant water channel (RD28, Daniels et al., 1994), do not.

The cysteine-scanning mutants examined in this study indicate that MIWC can be converted to a mercurial-sensitive water channel by creation of single cysteines at residues 70−73 and 189. Surprisingly, mutation MIWC A188C, which creates a cysteine at a position equivalent to C189 in CHIP28, did not confer mercurial sensitivity to MIWC; this finding is in agreement with data showing that mutation A210C in the brain MIWC isoform AQP-4 (equivalent to A188C in MIWC) did not confer mercurial sensitivity (Jung et al., 1994a). Similar results were also reported in cysteine mutation analysis of the RD28 plant water channel (Daniels et al., 1994). Another interesting observation here was that

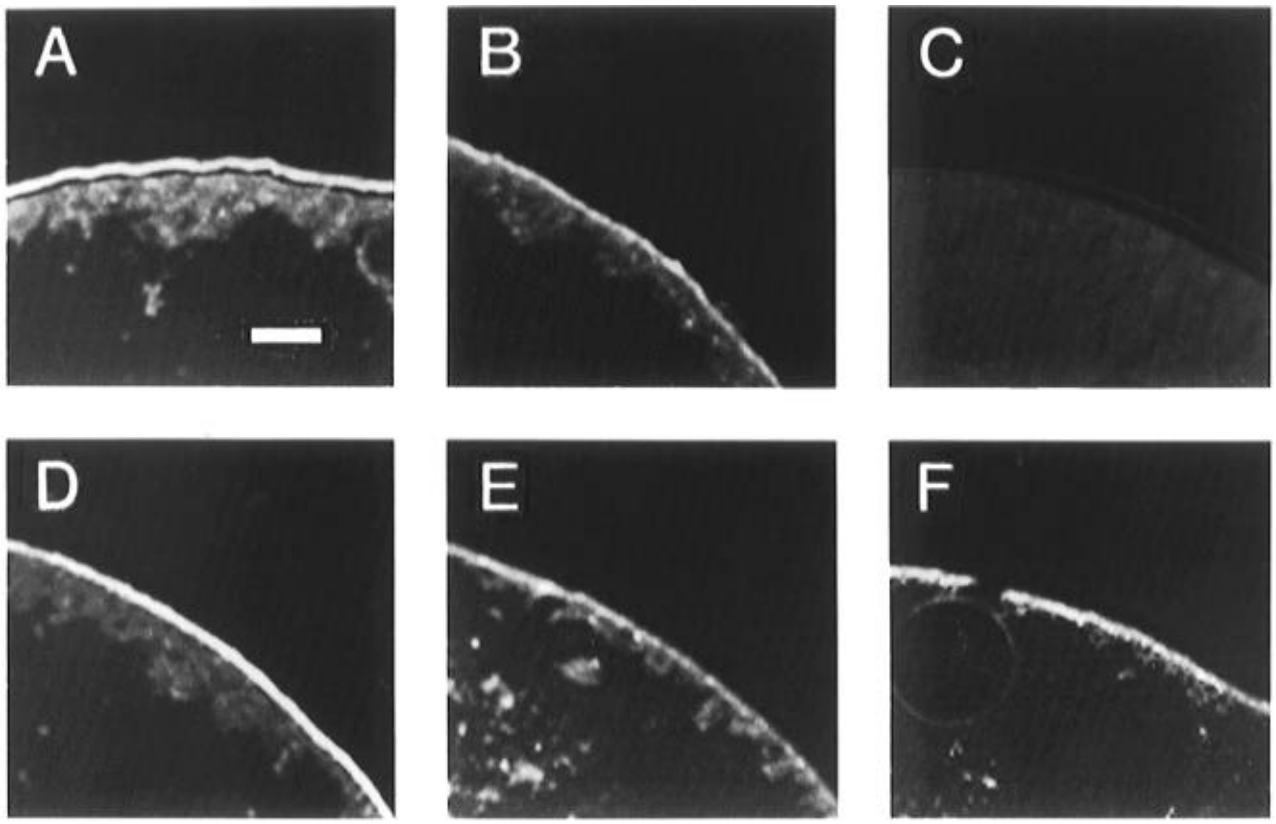

FIGURE 5: Immunofluorescence of oocytes expressing wild-type and various mutant MIWCs. Oocyte sections were immunostained with a rabbit polyclonal antibody raised against a synthetic C-terminus peptide of MIWC (see Materials and Methods). Images were recorded by a cooled CCD camera and copied by a video printer. Oocytes were injected with the cRNAs: 0.5 ng of wild-type MIWC (A), 0.125 ng of wild-type MIWC (B), water control (C), 0.5 ng of MIWC G72C (D), 0.5 ng of MIWC G72W (E), 0.25 ng of wild-type MIWC + 0.25 ng of G72W (F). Scale bar: 50 μm.

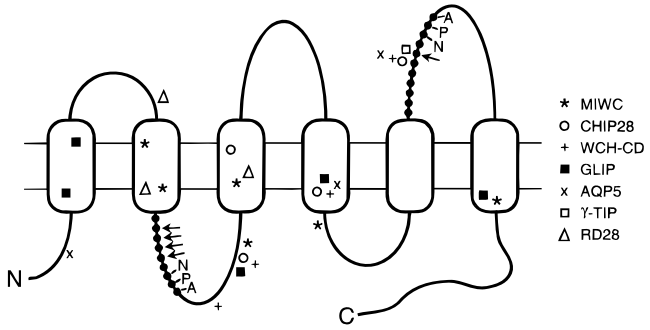

FIGURE 6: Locations of cysteine residues and NPA motifs in water-transporting proteins. Cysteine residues are denoted by specified symbols. Arrows indicate MIWC residues at which mutation to cysteine conferred mercurial sensitivity. See text for details.

two of the cysteine point mutants had remarkably higher sensitivity to $HgCl_2$ than native CHIP28. Taken together with the observations in Figure 6, the results indicate that insensitivity of MIWC to $HgCl_2$ is due to lack of cysteine residues at the critical regions of the MIWC molecule near the NPA sequences. The specific residues at which cysteine mutations confer mercurial sensitivity to MIWC may reside at or near the aqueous pore. This interpretation was supported by data showing that point tryptophan mutations in this region of the molecule block MIWC water permeability.

The regions of MIP family proteins near the NPA motifs have been proposed to be functionally important on the basis of their conservation in various related proteins from mammals, plants, bacteria, and yeast (Reizer et al., 1993). Secondary structure analysis suggested that these regions of the protein may form β-structure (van Hoek et al., 1993), and it has been proposed that these residues may dip into the membrane to form the water-selective pore of CHIP28 (Jung et al., 1994b). The results obtained here for MIWC support the view that the region just proximal to the NPA motifs may be at or near the MIWC aqueous pore. The observation that tryptophan point mutations block MIWC water permeability is consistent with physical blockade of the aqueous pathway by the relatively large amino acid tryptophan.

There are a number of caveats in the interpretation of site-directed mutagenesis studies of the type presented here, particularly because the MIWC protein has only one function, water transport, characterized by one intrinsic parameter, single channel water permeability. In contrast, for most ion channels, mutagenesis may affect multiple distinct parameters such as voltage dependence, open probability, unitary conductance, and inhibitor binding affinity. From the finding that MIWC water permeability is inhibited by tryptophan point mutations, it is not possible to distinguish between direct physical blockade of the aqueous channel and action of tryptophan at a distant site resulting in a change in protein conformation and decreased water permeability. The cysteine-scanning mutation studies support the possibility that the region of the protein just proximal to the NPA motifs is near the aqueous pore. It is recognized, however, that mercurial inhibition of water permeability conferred by a cysteine mutation may indicate accessibility of $HgCl_2$ to a created cysteine residue and/or action of $HgCl_2$ once bound. Because $HgCl_2$ and related compounds are relatively non-

specific for reaction with cysteines, it is not possible to readily determine whether $HgCl_2$ interacts with a created cysteine residue. Notwithstanding these caveats, the results here provide (a) an explanation for the mercurial insensitivity of MIWC, (b) evidence for a model of MIWC structure in which regions just proximal to the NPA motifs are involved in formation of the aqueous channel, and (c) evidence for functionally important interactions among MIWC monomers.

Several lines of evidence indicate that CHIP28 forms tetramers in membranes, including sedimentation studies (Smith & Agre, 1991), freeze-fracture electron microscopy (Verbavatz et al., 1993), image analysis of negatively stained two-dimensional crystals (Walz et al., 1994; Mitra et al., 1994), and cryoelectron crystallography (Mitra et al., 1995). Within CHIP28 tetramers, it is believed that individual monomers function independently on the basis of target size analysis (van Hoek et al., 1991), coexpression of wild-type and mutant CHIP28 monomers (Zhang et al., 1993b; Preston et al., 1993), and expression of heterodimers consisting of wild-type and mutant CHIP28 subunits (Shi et al., 1994). It has been assumed, but not yet shown, that related homologous proteins, including MIWC, are assembled as tetramers in membranes. It was found here that tryptophan mutants of MIWC (G72W and A188W) had a dominant-negative effect on the function of wild-type MIWC. Increasing amounts of the expressed tryptophan mutants remarkably decreased the water permeability conferred by expression of a constant amount of cRNA encoding wild-type MIWC. Immunofluorescence analysis indicated that the dominant-negative effect was due to a combination of decreased plasma membrane targeting of wild-type MIWC (or increased rate of MIWC degradation) together with decreased intrinsic (single channel) water permeability. The dominant-negative effect may potentially be exploited in the generation of transgenic animal models with decreased MIWC function. These results contrast with results for CHIP28 described above and suggest that monomeric MIWC subunits can interact functionally at the plasma membrane. However, because these mutant proteins may have structures different from wild-type MIWC, it cannot be concluded that functionally important subunit-subunit interactions occur between subunits of wild-type MIWC.

ACKNOWLEDGMENT

We thank Olivier Seksek for modification of image analysis routines, Alfred N. van Hoek for sequence alignments and hydropathy analyses, and William Skach and Javier Farinas for critical review of the manuscript.

REFERENCES

Agre, P., Preston, G. M., Smith, B. L., Jung, J. S., Raina, S., Moon, C., Guggino, W. B., & Nielsen, S. (1993) *Am. J. Physiol. 265*, F463−F476.

Daniels, M. J., Mirkov, T. E., & Chrispeels, M. J. (1994) *Plant Physiol. 106*, 1325−1333.

Deen, P. M., Verkijk, M. A., Knoers, N. V., Wieringa, B., Monnens, L. A., Van Os, C. H., & Van Oost, B. A. (1994) *Science 264*, 92−95.

Frigeri, A., Gropper, M. A., Umenishi, F., Kawashima, M., Brown, D., & Verkman, A. S. (1995a) *J. Cell Sci. 108*, 2993−3002.

Frigeri, A., Gropper, M. A., Turck, C. W., & Verkman, A. S. (1995b) *Proc. Natl. Acad. Sci. U.S.A. 92*, 4328−4331.

Fushimi, K., Uchida, S., Hara, Y., Hirata, Y., Marumo, F., & Sasaki, S. (1993) *Nature 361*, 549−552.

Hasegawa, H., Ma, T., Skach, W., Matthay, M., & Verkman, A. S. (1994) *J. Biol. Chem. 269*, 5497−5500.

Ishibashi, K., Sasaki, S., Fushimi, K., Uchida, S., Kuwahara, M., Saito, H., Furukawa, T., Nakajima, K., Yamaguchi, Y., Gojobori, T., & Marumo, F. (1994) *Proc. Natl. Acad. Sci. U.S.A. 91*, 6269−6273.

Jung, J. S., Bhat, R. V., Preston, G. M., Guggino, W. B., Baraban, J. M., & Agre, P. (1994a) *Proc. Natl. Acad. Sci. U.S.A. 91*, 13052−13056.

Jung, J. S., Preston, G. M., Smith, B. L., Guggino, W. B., & Agre, P. (1994b) *J. Biol. Chem. 269*, 14648−14654.

Ma, T., Frigeri, A., Hasegawa, H., & Verkman, A. S. (1994) *J. Biol. Chem. 269*, 21845−21849.

Maurel, C., Reizer, J., Schroeder, J. I., & Chrispeels, M. J. (1993) *EMBO J. 12*, 2241−2247.

Mitra, A. K., Yaeger, M., van Hoek, A. N., Wiener, M. C., & Verkman, A. S. (1994) *Biochemistry 33*, 12735−12740.

Mitra, A., van Hoek, A. N., Wiener, M., Yaeger, M., & Verkman, A. S. (1995) *Nat. Struct. Biol. 2*, 726−729.

Nielsen, S., Smith, B. L., Christensen, E. I., Knepper, M. A., & Agre, P. (1993) *J. Cell Biol. 120*, 371−383.

Preston, G. M., & Agre, P. (1991) *Proc. Natl. Acad. Sci. U.S.A. 88*, 11110−11114.

Preston, G. M., Jung, J. S., Guggino, W. B., & Agre, P. (1993) *J. Biol. Chem.* 268, 17−20.

Preston, G. M., Jung, J. S., Guggino, W. B., & Agre, P. (1994a) *J. Biol. Chem. 269*, 1668−1673.

Preston, G. M., Smith, B. L., Zeidel, M. L., Moulds, J. J., & Agre, P. (1994b) *Science 265*, 1585−1587.

Raina, S., Preston, G. M., Guggino, W. B., & Agre, P. (1995) *J. Biol. Chem. 270*, 1908−1912.

Reizer, J., Reizer, A., & Saier, M. H. (1993) *Crit. Rev. Biochem. Mol. Biol. 28*, 235−257.

Shi, L.-B., Skach, W., & Verkman, A. S. (1994) *J. Biol. Chem. 269*, 10417−10422.

Shi, L. B., Skach, W. R., Ma, T., & Verkman, A. S. (1995) *Biochemistry 34*, 8250−8256.

Skach, W., Shi, L.-B., Calayag, M. C., Frigeri, A., Lingappa, V. R., & Verkman, A. S. (1994) *J. Cell Biol. 125*, 803−815.

Smith, B. L., & Agre, P. (1991) *J. Biol. Chem. 266*, 6407−6415.

Van Hoek, A. N., Hom, M. L., Luthjens, L. H., de Jong, M. D., Dempster, J. A., & van Os, C. H. (1991) *J. Biol. Chem. 226*, 16633−16635.

Van Hoek, A. N., Wiener, M., Bicknese, S., Miercke, L., Biwersi, J., & Verkman, A. S. (1993) *Biochemistry 32*, 11847−11856.

Van Os, C. H., Deen, P. M. T., & Dempster, J. A. (1994) *Biochim. Biophys. Acta 1197*, 291−309.

Verbavatz, J. M., Brown, D., Sabolic, I., Valenti, G., Ausiello, D. A., van Hoek, A. N., Ma, T., & Verkman, A. S. (1993) *J. Cell Biol. 123*, 605−618.

Verkman, A. S., van Hoek, A. N., Ma, T., Frigeri, A., Skach, W. R., Mitra, A., Tamarrappoo, B. K., & Farinas, J. (1996) *Am. J. Physiol. 270* (in press).

Walz, T., Smith, B. L., Zeidel, M. L., Engel, A., & Agre, P. (1994) *J. Biol. Chem. 269*, 1383−1386.

Yang, B., Ma, T., & Verkman, A. S. (1995) *J. Biol. Chem. 270*, 22907−22913.

Zen, K., Biwersi, J., Periasamy, N., & Verkman, A. S. (1992) *J. Cell Biol. 119*, 99−110.

Zhang, R., Logee, K., & Verkman, A. S. (1990) *J. Biol. Chem. 265*, 15375−15378.

Zhang, R., Skach, W., Hasegawa, H., van Hoek, A. N., & Verkman, A. S. (1993a) *J. Cell Biol. 120*, 359−369.

Zhang, R., van Hoek, A. N., Biwersi, J., & Verkman, A. S. (1993b) *Biochemistry 32*, 2938−2941.

BI9520038